ACS Chemical Neuroscience

pubs.acs.org/chemneuro Research Article

Targeting Two-Pore-Domain Potassium Channels by Mechanical Stretch Instantaneously Modulates Action Potential Transmission in Mouse Sciatic Nerves

Jia Liu, Nishanth Ganeshbabu, Noha Shalaby, Longtu Chen, Tiantian Guo, and Bin Feng*

Cite This: *ACS Chem. Neurosci.* 2021, 12, 3558−3566 Read Online

ACCESS | Metrics & More | Article Recommendations

ABSTRACT: Recent reports indicate dominant roles of TRAAK and TREK-1 channels, i.e., mechanosensitive two-pore-domain potassium channels (K2P) at the nodes of Ranvier for action potential repolarization in mammalian peripheral nerves. Functional changes in mammalian peripheral nerve conduction by mechanical stretch studied by recording compound action potentials lack the necessary resolution to detect subtle neuromodulatory effects on conduction velocity. In this study, we developed a novel *in vitro* approach that enables single-fiber recordings from individual mouse sciatic nerve axons while delivering computer-controlled stepped stretch to the sciatic nerve trunk. Axial stretch instantaneously increased the conduction delay in both myelinated A-fibers and unmyelinated C-fibers. Increases in conduction delay linearly correlated with increases in axial stretch ratio for both A- and C-fibers. The slope of the increase in conduction delay versus stretch ratio was steeper in C-fibers than in A-fibers. Moderate axial stretch (14−19% of *in vitro* length) reversibly blocked 37.5% of unmyelinated C-fibers but none of the eight myelinated A-fibers tested. Application of arachidonic acid, an agonist to TRAAK and TREK-1 to sciatic nerve trunk, blocks axonal transmission in both A- and C-fibers with delayed onset and prolonged block. Also, the application of an antagonist ruthenium red showed a tendency of suppressing the stretch-evoked increase in conduction delay. These results could draw focused research on pharmacological and mechanical activation of K2P channels as a novel neuromodulatory strategy to achieve peripheral nerve block.

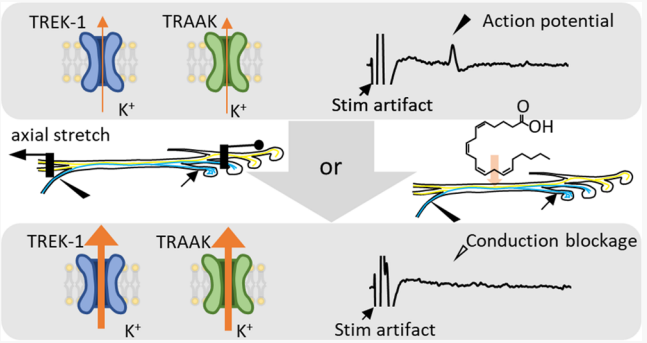

KEYWORDS: *Sciatic nerve, conduction block, two-pore domain potassium channel, neuromodulation, mechanosensitive channel, single-fiber recording*

INTRODUCTION

Blocking action potential (AP) transmission in peripheral nerves effectively suppresses pain arising from the periphery without causing adverse off-target effects on the central nervous system.[1,2] Targeting peripheral nerves can avoid effects like tolerance and addiction that underlie the current epidemic of prescription opioid abuse in the USA. Blocking AP transmission in peripheral nerves can also potentially treat chronic disorders like obesity (the vagus nerve),[3,4] heart failure (sympathetic nerves),[5] and insufficient bladder voiding (the pudendal nerves).[6] Despite centuries of research, the exact composition of ion channels that participate in AP transmission in mammalian peripheral nerves remains undetermined. Recently, Kanda et al. and Brohawn et al. independently reported convincing evidence from patch-clamp studies on the nodes of Ranvier (NRs) of mammalian peripheral nerves.[7,8] Both reports indicate the unexpected role of two-pore domain potassium channels (K2P), not voltage-gated potassium channels, in dominating AP repolarization at the NRs of mammalian peripheral nerves.

The study by Kanda et al. showed that 87% and 91% of mouse NRs are immunopositive for TREK-1 and TRAAK, respectively,[7] two ion channels that belong to the family of 15 K2P channels.[9] TREK-1 and TRAAK extensively coexpress and form heteromeric TREK-1/TRAAK channels as well as homomeric TREK-1 and TRAAK channels in the NRs.[7] In addition, TREK-1 and TRAAK are abundantly expressed in afferent neurons innervating the colon and rectum,[10] the vast majority of which are unmyelinated C-fibers without NRs.[11]

Received: January 27, 2021
Accepted: August 12, 2021
Published: August 22, 2021

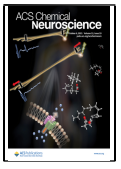

Known as the "leak channels" in the classic Hodgkin−Huxley formulation of AP generation, K2P channels are generally not gated by membrane voltage but by other mechanisms like mechanical stretch, temperature, oxygen, and pH (see ref 9 for a comprehensive review). Specifically, TRAAK and TREK-1 are prominently gated by temperature and mechanical stretch. TREK-1 was the first mechanosensitive potassium channel to be recognized, which is also thermosensitive with a 20-fold increase in activity when temperature rises from 22 to 42 °C.[12−14] TRAAK is also mechanosensitive and thermosensitive,[15] showing a 12- to 20-fold increase in activity when temperature rises from 17 to ∼40 °C.[16] For both TREK-1 and TRAAK, maximal activity is reached between 37 and 42 °C and activity falls sharply at higher or lower temperatures.[17]

The temperature gating of TREK-1 and TRAAK channels is consistent with prior findings of conduction block in mammalian myelinated axons by local cooling of the nerve to below 16 °C [18,19] or by local heating to over 46 °C;[20,21] the cold and hot temperature ranges in which TREK-1 and TRAAK channels are strongly inhibited.[17] A recent study reported peripheral nerve block by a combination of low and high temperatures,[22] which further confirms the findings by Kanda et al. that TREK-1 and TRAAK are pivotal for AP transmission in myelinated mammalian peripheral axons. Since TREK-1 and TRAAK are also mechanosensitive, it is conceivable that axial mechanical stretch of peripheral nerves can also profoundly modulate AP transmission. A handful of prior studies recorded compound action potentials (CAP) from mammalian nerves and reported reduced CAP magnitude following mechanical nerve elongation.[23−27] In this study, we developed a novel experimental approach that enabled stable and robust single-fiber recordings from individual mouse sciatic nerve axons while delivering computer-controlled axial mechanical stretch to the nerve trunk. We showed instantaneous decreases in nerve conduction velocity (CV) even by moderate axial mechanical stretch (<3%) in both myelinated A-fibers and unmyelinated C-fibers and reversible blockade of AP transmission in a portion of axons at axial stretch beyond 14%, which are likely attributed to the mechanical gating of TREK-1 and TRAAK channels. In addition to mechanical stretch, we showed that activating these K2P channels by pharmacological agonists also reversibly blocked AP transmission in sciatic axons, whereas K2P antagonists had no significant effects.

RESULTS AND DISCUSSION

AP transmission in individual mouse sciatic axons was recorded by single-fiber recordings once every 2 s while applying stepped axial stretch to the sciatic nerve trunk. Displayed in Figure 1A are two typical single-fiber recordings from a fast-conducting A-fiber (CV > 1 m/s [28,29] before stretch) and a slow-conducting C-fiber (CV < 1 m/s before stretch) recorded before and after axial sciatic stretch. The conduction delays (CD) from both fibers were plotted as scattered dots in Figure 1B during a typical stepped stretch protocol (60 s step with 5 s ramped rising and returning phases). The increase in CD was instantaneous upon the onset of stretch, and the CD returned to baseline immediately after the stretch. Displayed in Figure 1C are the CDs recorded from a typical axon undergoing ascending steps of sciatic axial stretch (60 s step with 5 s rising and returning ramps, 0.5−5 mm at 0.5 mm/step). For this fiber, 5 mm stretch evoked a

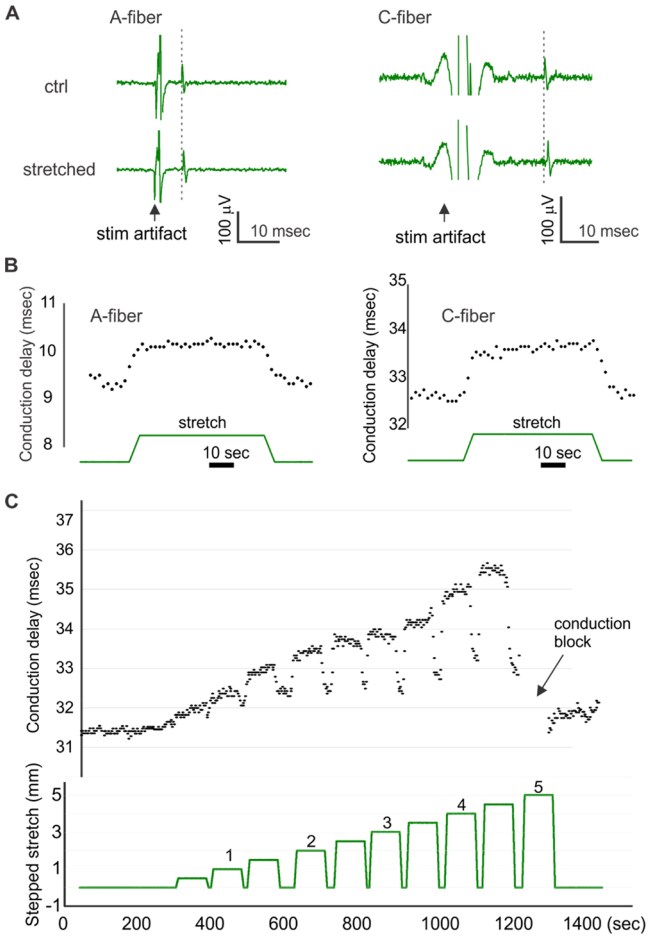

Figure 1. Axial nerve stretch instantaneously increases the conduction delay (CD) of sciatic axons (i.e., decreasing the conduction velocity). Displayed in (A) are typical single-fiber recordings from a myelinated A-fiber and an unmyelinated C-fiber prior to and after axial stretch. Notice that greater electrical stimulus intensity is generally required to evoke action potentials in a C-fiber,[29] which leads to a more pronounced stimulus artifact than for A-fibers. CD was recorded at 0.5 Hz and plotted during the course of a stepped stretch protocol in (B). A typical fiber was tested with ascending levels of the stepped axial stretch as shown in (C).

reversible conduction block as indicated by the arrow in Figure 1C.

The CD at each stretch step was quantified by averaging five consecutive CDs 3 s after the onset of each stepped stretch. Variation of CD within each stepped stretch was considered negligible as the coefficient of variation was found to be less than 0.2%. Stretch ratio was calculated by dividing the stretched nerve length with the zero-stretch nerve length (i.e., the *in vitro* length). In Figure 2A, the percentage increases in CD from 10 myelinated A-fibers and 12 unmyelinated C-fibers were plotted against stretch ratio, which follows a linear relationship. For each fiber, the % CD increase was linearly fitted with the stretch ratio; R^2 values were 0.95 ± 0.01 for the 10 A-fibers and 0.96 ± 0.01 for the 12 C-fibers. As shown in Figure 2B, the slope of % CD increase versus stretch ratio was significantly greater in C-fibers than in A-fibers (*t* test, p = 0.011), indicating a stronger decrease in the CV in unmyelinated C-fibers by axial nerve stretch.

Displayed in Figure 3 is a typical example of the reversible conduction block in a C-fiber by axial sciatic stretch. The raw

https://doi.org/10.1021/acschemneuro.1c00052
ACS Chem. Neurosci. 2021, 12, 3558−3566

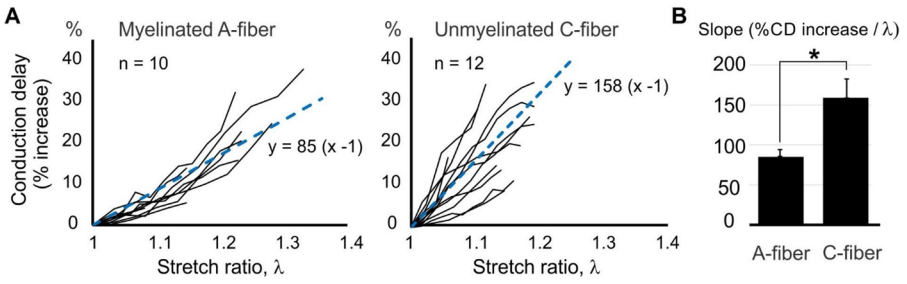

Figure 2. Linear increase in conduction delay (CD) with increase in axial stretch ratio of sciatic nerve trunk in both A- and C-fibers. (A) Percentage increase in CD was plotted against stretch ratio for 10 A-fibers and 12 C-fibers. (B) The slope of % CD increase versus stretch ratio is significantly greater in C-fibers than in A-fibers. *$p < 0.05$.

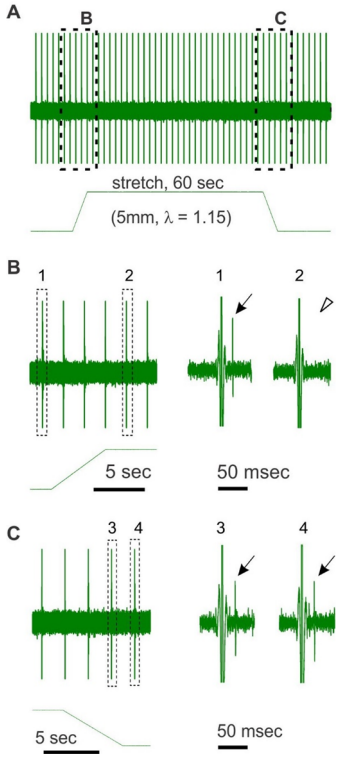

Figure 3. Reversible conduction block by axial stretch in some sciatic axons. (A) Typical single-fiber recording from an unmyelinated C-fiber during a stepped sciatic stretch protocol. (B) Extended view of the ramped rising phase of the stepped stretch in (A). (C) Extended view of the ramped returning phase of the stretch in (A). Action potentials were denoted with black arrows, and the absence of an action potential due to conduction block was denoted with an open arrowhead.

single-fiber recording data and stepped stretch were plotted in Figure 3A with magnified views in time scale plotted in Figure 3B,C. AP transmission was completely blocked at the onset of the stepped stretch, remained blocked throughout the stepped stretch, and instantaneously recovered following the ramped reduction of stretch. Among the eight C-fibers tested with stretch up to 5 mm, three (37.5%) showed reversible block at 5 mm stretch. Of the 10 total A-fibers, eight were stretched to 5 mm (two fibers experienced mechanical failure at one of the ligatures or loss of single-fiber recording signals at 5 mm stretch), and none of the eight fibers showed conduction block. Among the five A-fibers tested with stretch beyond 7 mm (but no more than 8 mm to avoid disrupting single-fiber recordings), one (20%) showed reversible block at 7 mm stretch.

The role of K2P channels in the conduction block is further confirmed by the application of K2P agonist (arachidonic acid, AA), antagonist (ruthenium red, RR), and 2% lidocaine as a positive control in single-fiber recordings. Pharmacological reagents were perfused locally to the middle portion of the intact sciatic nerve trunk at 100 μL/min for 15 min. Among the 32 axons treated by 5 mM AA, CV in six axons was irreversibly blocked and could not be washed back within 25 min. Considering possible neuronal damage, we excluded these six axons in subsequent analysis (i.e., $n = 26$ for 5 mM AA). As shown with typical recordings in Figure 4A, both lidocaine (2%) and agonist AA (5 mM) reversibly blocked sciatic nerve conduction whereas neither antagonist RR (0.5 mM) nor a lower concentration of AA (0.5 mM) did. The representative pharmacological effect on the axonal CD is shown in Figure 4B, in which CD was measured once every 2 s for up to 40 min. There were delayed onsets of the block following the start of perfusion and prolonged block after terminating the perfusion. The axonal CV relative to baseline (t_0 in Figure 4B) after reagents application (t_1 in Figure 4B) and after washout (t_2 in Figure 4B) was summarized in Figure 4C (CV = 0 indicates complete nerve block). Lidocaine (2%) blocked conduction ($n = 4$, Kruskal–Wallis one-way ANOVA on ranks, $H = 10.586$, SNK post hoc comparison, $p = 0.005$ for t_1 vs t_0), and so did 5 mM AA ($n = 26$, Kruskal–Wallis one-way ANOVA on ranks, $H = 47.793$, SNK posthoc comparison, $p < 0.001$ for t_1 vs t_0). CV was not completely washed back to control level after lidocaine ($p = 0.021$ for t_2 vs t_0) or 5 mM AA application ($p < 0.001$ for t_2 vs t_0). In contrast, neither RR nor 0.5 mM AA had any significant effect on CV ($n = 15$, $H = 0.261$, $p = 0.878$ for RR; $n = 3$, $H = 0.204$, $p = 0.800$ for 0.5 mM AA).

Displayed in Figure 5A is the distribution of conduction velocities in 26 axons tested with 5 mM AA, indicating that nerve conduction in 50% C-fibers and 75% A-fibers was completely blocked by 5 mM AA. Among the axons blocked by 5 mM AA, the delayed onset and prolonged block time are summarized in Figure 5B, showing significantly greater onset delay in C-fibers than in A-fibers (t test, $p = 0.0426$) whereas the prolonged block time was comparable between the fiber types. It is noted that Figure 5B includes only six of the seven blocked C-fibers due to loss of continuous recording from one of the C-fibers in the washout phases.

The role of TREK-1 and TRAAK in stretch-evoked increase in CD was further tested by applying agonist AA or antagonist RR on unmyelinated C-fibers before and after the axial stretch protocol. To avoid excessive mechanical damage, the

https://doi.org/10.1021/acschemneuro.1c00052
ACS Chem. Neurosci. 2021, 12, 3558–3566

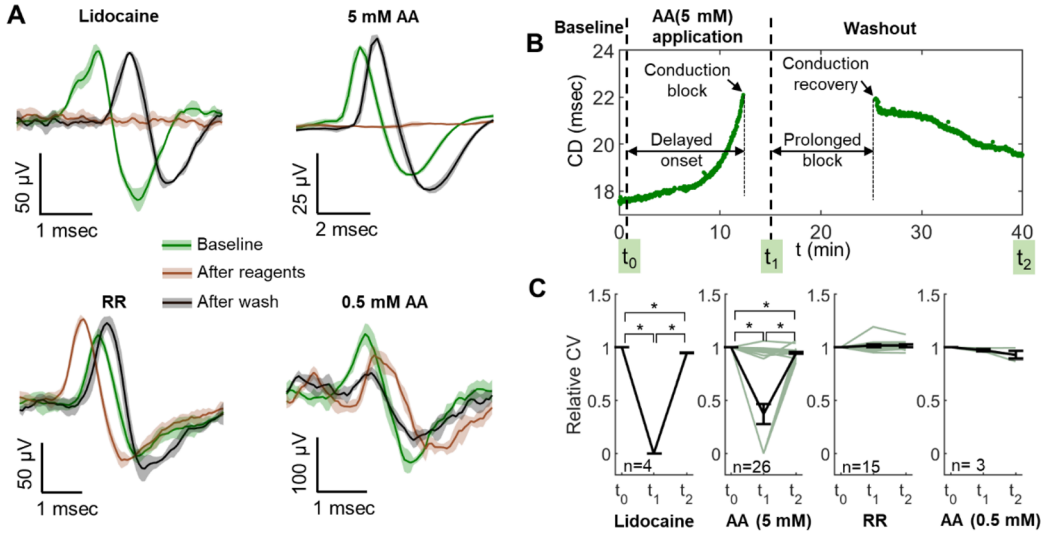

Figure 4. Conduction block by pharmacological targeting of K2P channels. (A) Single-fiber action potentials (APs) recorded before (baseline) and after reagent application and 25 min after wash. Each trace is presented as the mean (solid line) ± SE (shadowed area) from five consecutive APs. (B) Representative recordings of pharmacological effect (i.e., 5 mM AA) on conduction delay (CD) in a single-fiber recording. CD was measured once every 2 s for up to 40 min. Delayed onset is defined as the time period between the start of reagent application and the start of AP conduction block. The prolonged block is defined as the time period between terminating the reagent application and conduction recovery. t_0 and t_1 refer to the start and end of the reagent application, and t_2 is the time of complete washout. (C) Relative conduction velocity (CV) (normalized by baseline) before (t_0) and after reagent application (t_1) and 25 min after wash (t_2). Black lines are the mean ± SE. Green lines are relative CV from individual axons.

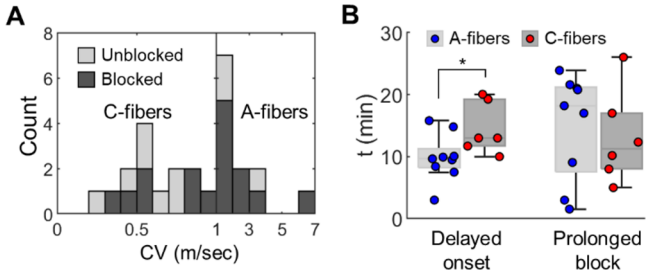

Figure 5. Both A- and C-type sciatic axons were blocked by 5 mM AA. (A) Distribution of baseline conduction velocity (CV) of 26 sciatic axons tested with 5 mM AA. Nine of the 12 A-fibers and 7 of the 14 C-fibers were blocked by 5 mM AA. (B) Delayed onset and prolonged block time in 9 A-fibers and 6 C-fibers blocked by 5 mM AA.

maximum axial stretch was limited to 3 mm. Displayed in Figure 6A is the % increase in CD versus stretch ratio from six unmyelinated C-fibers before (baseline), immediately after (RR) and 25 min after (washout) RR application (0.5 mM). The increase in CD from each afferent was linearly fitted with the stretch ratio showing R^2 value of 0.95 ± 0.02 for the baseline group, 0.95 ± 0.03 for RR treatment, and 0.97 ± 0.01 for washout. The TREK-1 and TRAAK antagonist RR significantly decreased the slope of the increase in CD versus stretch ratio (paired t test, p = 0.044). Similarly, displayed in Figure 6B is the effect of agonist AA on another six unmyelinated C-fibers before (baseline), immediately after (AA), and 25 min after (washout) AA application (5 mM). Application of agonist AA slightly but not significantly increased the slope of the % increase in CD versus stretch ratio relations. The slope after washout is significantly lower than that after AA application (paired t test, p = 0.019).

To the best of our knowledge, this is the first study that reported continuous recordings of single-fiber APs from mammalian peripheral nerves during the course of axial nerve stretch. The effect of axial stretch to induce trauma in mammalian peripheral nerves was studied previously by extracellular recordings of CAP, showing progressive reduction of CAP amplitude when axial nerve stretch was beyond a certain threshold (5% for ref 26, 6% for refs 23, 27, and 25, and 8.3% for ref 24). CAP measures the spatial and temporal summation of electrical potentials from a population of peripheral axons, which is not exclusively determined by the number of recorded axons. Other factors can also profoundly impact the amplitude of CAP, especially during axial mechanical stretch, including the relative distance between the axon and recording electrode, the impedance change of the insulating connective tissue layers, and even the change of electrode impedance due to altered local electrolyte conditions. Indeed, variations in amplitude are common in extracellular recordings from peripheral nerve axons, especially over minutes-long recordings.[30,31] In addition, most prior studies were conducted *in vivo* or *ex vivo* with intact circulation, and axial nerve stretch reportedly decreases intraneural blood circulation, which is known to affect nerve function.[23,32,33] In contrast, we implemented *in vitro* single-fiber recordings in the current study and focused on the temporal CD of individual peripheral axons as a robust and sensitive metric to assess the effect of axial nerve stretch. We previously demonstrated that the temporal CD from *in vitro* single-fiber recordings was robust and repeatable for hours[30] and enabled the detection of the subtle neuromodulatory effects of ultrasound on peripheral axons.[31] To minimize the effect of axial displacement on nerve stimulation and recording conditions, we designed our *in vitro* setup to stimulate and record not the sciatic nerve trunk, like in most prior studies, but at distal and proximal branches, respectively. We managed to keep the sural and L5 spinal branches in loose condition throughout the axial stretch protocol. The loose configuration of the nerve branches allows movement of the stimulating and recording electrode by

https://doi.org/10.1021/acschemneuro.1c00052
ACS Chem. Neurosci. 2021, 12, 3558−3566

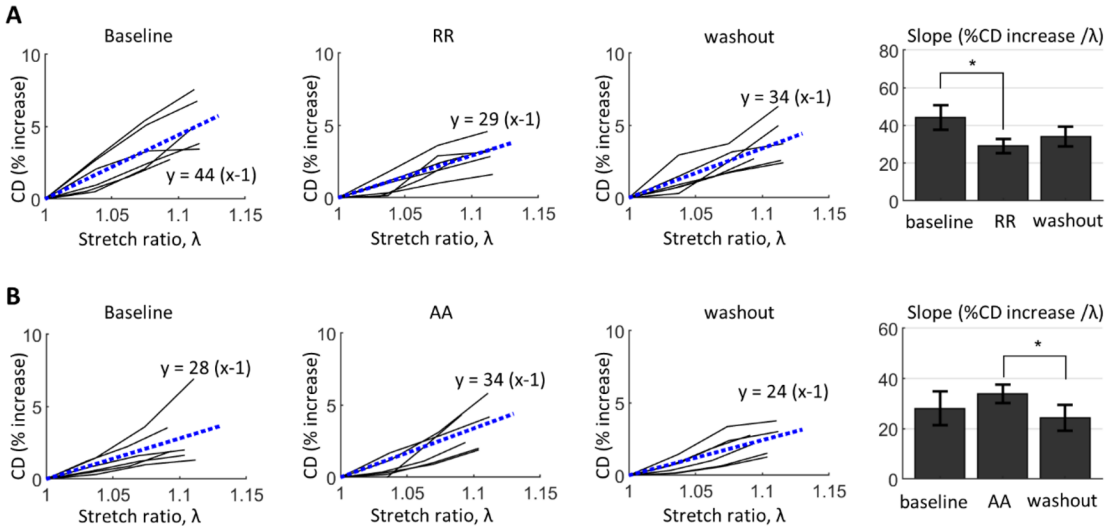

Figure 6. Effect of TREK-1 and TRAAK antagonist (RR) and agonist (AA) on the axial stretch-induced increase in conduction delay (CD). The % increase in CD versus stretch ratio was recorded before (baseline), immediately after, and 25 min after (washout) the application of either RR (0.5 mM) or AA (5 mM). (A) Application of antagonist RR significantly reduced the slope of the % increase in CD versus stretch ratio relations. (B) Application of agonist AA slightly increased the slope with no statistical significance. The slope after washout was significantly lower than immediately after AA application.

millimeters without causing apparent mechanical strain, and this amount of movement was verified not to affect the single-fiber recordings of CD (data not shown).

From single-fiber recordings, we observed a continuous and linear increase of nerve CD in both myelinated A-fibers and unmyelinated C-fibers in mouse sciatic nerve. This is consistent with a previous report with CAP recordings from A-fibers showing 20% stretch caused a significant increase in conduction latency.[26] However, the CAP recordings were unable to detect any significant changes in conduction latency at lower axial stretch levels. As shown in Figure 1A, fast conducting A-fibers showed submillisecond changes in CD in mouse sciatic nerve during stretch, which may have escaped detection in CAP recordings. The absence of changes in conduction latency reported previously[26] likely reflects the low sensitivity of CAP recordings in detecting changes in CD. A significant observation of the current study is the continuous increase in CD with axial stretch in myelinated A-fibers, in which transmission of APs is saltatory at the NRs, and thus the CV was assumed not to be affected by nerve elongation.[26] In addition, the increase in CD is virtually instantaneous, showing almost no latency, which strongly indicates mechanical modulation as the dominant factor rather than slower effects like chemical ligand binding or second messenger cascade. The increase in CD needs to take place at the depolarization phase of AP generation in the NRs. Thus, mechanosensitive ion channels of TRAAK and TREK-1 widely present at NRs are logical candidates for the instantaneous CD increases via axial mechanical stretch. Indeed, prior patch-clamp studies indicated TRAAK and TREK-1 channels remained open under sustained mechanical stretch and showed minimal desensitization to stretch.[15,34] Presumably, under stepped axial nerve stretch, TRAAK and TREK-1 channels can remain constitutively open to provide an increased potassium current that counters the sodium depolarization at the NRs, which leads to a reduced rate of depolarization and an increase in CD. The fact that TRAAK and TREK-1 are gradually gated by mechanical stretch is also consistent with the current report of a gradual increase in CD with increased nerve stretch ratio in A-fibers.

Similar to A-fibers, our results also showed progressive increase in CD in unmyelinated C-fibers following axial nerve stretch; the rate of CD increase is even greater in C-fibers than in A-fibers. The increase in CD to stretch in C-fibers is also instantaneous, suggesting a mechanical event. In contrast to the recent reports of TREK-1 and TRAAK at NRs of myelinated axons,[7,8] we still have limited knowledge on the spatial distribution of TREK-1 and TRAAK in unmyelinated axons. A study by La et al. showed that TREK-1 and TRAAK channels are widely expressed in visceral afferents innervating the colon,[10] which are predominantly unmyelinated C-fibers.[11] Thus, TREK-1 and TRAAK channels are likely present in unmyelinated sensory afferents. Collectively, results by us and others strongly suggest the role of TREK-1 and TRAAK in regulating AP transmission in unmyelinated C-fibers. More importantly, 37.5% of C-fibers showed reversible conduction block at 5 mm stretch (14−19% stretch of *in vitro* length). In contrast, none of the myelinated A-fibers were blocked by 5 mm stretch. Excessive stretch over ∼25% reportedly caused permanent structural damage to peripheral nerves,[23,32] which is beyond the scope of this study. The nerve block by stretch in unmyelinated C-fibers as shown in Figure 3 is instantaneous with the onset of stretch. Recovery from nerve block is also instantaneous right after removing the stretch. In addition, the conduction block was maintained throughout the stepped stretch. These blocking kinetics to stretch agree well with the mechanical gating kinetics of TRAAK and TREK-1 channels,[15,34] which strongly suggests critical roles for TRAAK and TREK-1 channels in C-fiber conduction block by axial stretch.

We provided convincing pharmacological data to further support the role of K2P channels in conduction block in sciatic nerves. To avoid interfering with the nerve conduction, we did not inject the reagents into the nerve trunk but applied local perfusion from outside the epineurium. The perfusion rate of 100 μL/min was validated to effectively deliver reagents to sciatic axons by 2% lidocaine, a concentration used routinely in the clinic for peripheral nerve block.[35] We showed that activating K2P by agonist AA (5 mM) blocked nerve conduction in 50% C-fibers and 75% A-fibers, consistent

https://doi.org/10.1021/acschemneuro.1c00052
ACS Chem. Neurosci. 2021, 12, 3558−3566

with our results of activating K2P by axial mechanical stretch. In contrast, blocking the K2P by antagonist RR did not lead to nerve conduction block, which might be due to the presence of other potassium channels in peripheral axons that also contribute to the repolarization of APs. The 5 mM concentration of AA and 0.5 mM concentration of RR used in the current study is ∼1000 times their respective half maximal effective concentration (EC_{50}) for binding with TRAAK and TREK-1; a lower concentration of 0.5 mM AA failed to block conduction. It is worth mentioning that perineurium functions as a blood−nerve barrier[36] with tight-junction proteins to limit diffusion.[36] We reported previously that concentrations 3 orders higher than EC_{50} were required to deliver sodium channel blockers across the tight junction of colonic mucosa.[37,38] Thus, the use of 5 mM AA and 0.5 mM RR is required when delivering from outside the sciatic epineurium. The delayed onset and prolonged block due to 5 mM AA (over 5 min) likely reflect the diffusion process for reaching the axons inside the endoneurium. However, there is no significant correlation between delayed onset and prolonged block (R^2 = 0.03 for A-fibers, R^2 = 0.24 for C-fibers), indicating that the diffusion barrier is not the sole factor that determines the prolonged block. In addition, we tested the axial stretch protocol before and after application of agonist AA or antagonist RR in unmyelinated C-fibers. Our finding that antagonist RR attenuates the slope of % increase in CD versus stretch ratio relations and agonist AA slightly enhances the slope provides further support that axial stretch modulates the action potential transmission through TRAAK or TREK-1 channels. It is noted that nerve stretch potentially leads to reduced axonal diameter, the extent to which remains undetermined experimentally. Assuming constant axonal volume, stretch-induced decrease in axonal diameter alone will lead to significant increase in conduction delay according to the core-conductor model of action potential transmission.[39] Further experimental evidence is needed to differentiate the proportions of stretch-induced increase in conduction delay caused by reduced axonal diameter versus by activation of K2P channels.

The finding of selective nerve block of unmyelinated C-fibers by moderate axial stretch (14−19% of *in vitro* length) has profound implications for peripheral neuromodulation. Prior biomechanical studies indicate that peripheral nerves in the *in vivo* situation are prestretched by 11 ± 1.5% of their *in vitro* length.[23] Thus, the 14−19% *in vitro* stretch correlates to approximately 3−8% of *in vivo* axial stretch, which is a moderate stretch level without causing apparent impairment of venular blood flow.[32] In pathophysiological conditions, C-fibers play critical roles and are often responsible for the persistence of a diseased state.[40] For example, C-fiber nociceptors (afferents that encode tissue-injurious stimuli and commonly initiate the sensation of pain) can sensitize to drive the persistence of many chronic pain conditions.[41−44] Selective targeting of unmyelinated C-fibers by moderate axial stretch could potentially block sensitized C-fibers while sparing A-fibers for normal physiological functions. Thus, the current report could draw focused research on mechanical axial stretch as a novel neuromodulatory strategy to achieve selective peripheral nerve block.

MATERIALS AND METHODS

All experiments were reviewed and approved by the University of Connecticut Institutional Animal Care and Use Committee.

Harvesting Mouse Sciatic Nerve Trunk and Branches. Sciatic nerves were harvested from male or female C57BL/6 mice 8−12 weeks of age, 20−30 g body weight (Taconic, Germantown, NJ). Mice were anesthetized by isoflurane inhalation, euthanized by exsanguination via perforating the right atrium, and transcardially perfused with ice-cold oxygenated (95% O_2, 5% CO_2) Krebs solution containing (in mM) 117.9 NaCl, 4.7 KCl, 25 $NaHCO_3$, 1.3 NaH_2PO_4, 1.2 $MgSO_4$, 2.5 $CaCl_2$, and 11.1 D-glucose. The mouse carcass was transferred to a dissection chamber filled with ice-cold oxygenated Krebs solution, where both sciatic nerve trunks and branches (∼30 mm) were harvested bilaterally from the L3−L5 entry points to the spinal cord to the distal branches of sural, common peroneal, and tibial nerves. Sciatic nerve trunks and branches were then transferred to a custom-built perfusion compartment containing a tissue chamber superfused with oxygenated Krebs solution at 30−32 °C and an adjacent mineral oil chamber for single-fiber recordings.

Axial Mechanical Stretch of Mouse Sciatic Nerve Trunk. As shown in Figure 7, the proximal L3 and L4 spinal nerves were ligated

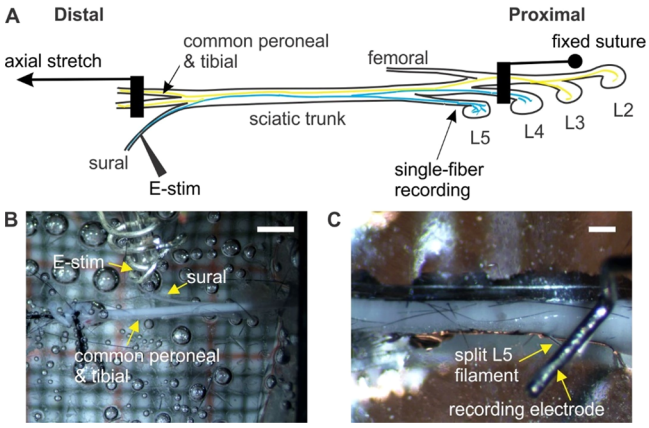

Figure 7. A novel single-fiber recording setup to assess axial nerve stretch effect on action potential transmission in mouse sciatic nerves. As schematized in (A), mechanical tensile stretch was delivered by ligating the proximal L3 and L4 spinal nerves and distal common peroneal and tibial nerves. Action potentials were evoked from the sural nerve by a suction electrode at 0.5 Hz as shown in the photograph in (B) and recorded from split filaments of the L5 spinal nerve as shown in (C). The scale bars are approximately 2 mm in (B) and 0.2 mm in (C).

with fine silk suture (Ethicon 6.0, Advanced Sterilization Products, Irvine, CA) as were the distal common peroneal and the tibial nerves. The ligatures were 22−35 mm apart, and the nerve length in between was measured prior to tensile stretch. The end of the proximal ligature (L3 and L4 spinal nerves) was pinned and fixed; the distal ligature connecting the common peroneal and tibial nerves was stretched by a computer-controlled force and displacement actuator (300D, Aurora Scientific Inc., ON, Canada). The nerve was prestretched slightly by a ∼10 mN axial force to remove any slack, a configuration considered as zero stretch state. The 10 mN axial force generates negligible axial strain according to a previous study,[23] and thus we consider the measured nerve length as the *in vitro* length. The stepped stretch protocol consisted of a ramped rising phase from zero stretch to target stretch in 5 s, a maintenance phase for 60 s, and a ramped return phase to zero stretch in 5 s. Multiple stretch steps (0.5−5 mm in 0.5 mm steps) were delivered to assess the effect of stretch on both unmyelinated C-fibers and myelinated A-fibers. In some experiments, recordings were disrupted before completing the stretch steps, which was usually due to mechanical failure at one of the ligatures or loss of single-fiber recording signals. In some recordings from A-fibers, mechanical stretch beyond 5 mm was delivered with 1 mm steps up to 8 mm.

Single-Fiber Recordings from Sciatic Axons during Axial Stretch. The proximal branches of the sciatic nerve (i.e., the L3−L5

https://doi.org/10.1021/acschemneuro.1c00052
ACS Chem. Neurosci. 2021, 12, 3558−3566

spinal nerves) were pulled into the adjacent, mineral oil-filled recording chamber. The L5 spinal nerve was carefully desheathed and intricately split into fine filaments of 10−20 μm thick, each of which was mounted onto a custom-built platinum−iridium recording electrode (⌀100 μm) for extracellular single-fiber recordings following a procedure reported previously.[38,45,46]

APs were evoked by electrically stimulating the sural nerve (i.e., a distal branch of the sciatic nerve) with axon projections to the L5 spinal nerve (Figure 7A). To continuously monitor the effect of axial nerve stretch, we evoked and recorded APs repeatedly every 2 s, a frequency low enough to avoid the activity-dependent slowing in unmyelinated C-fibers based upon our prior reports.[30,31] To minimize stimulus artifact, we used a suction electrode fabricated from a quartz glass capillary to deliver monopolar cathodal current pulses (0.2−3 mA, 0.2 ms duration, 0.5 Hz). The electrical current that travels through the surrounding Krebs bath solution to the recording electrode is a key contributor to the stimulus artifact, which could be minimized by increasing the access resistance between the suction stimulating electrode and bath solution via applying a gentle suction to "seal" the electrode tip with the epineurium.

Movement between nerve and electrodes is detrimental to extracellular single-fiber recordings. To address that, we only applied axial stretch to the sciatic nerve trunk while keeping the branches for recording (L5 spinal nerve) and stimulating (sural nerve) loose and stretch-free. Both recording and stimulating electrodes were mounted onto micromanipulators (no. 640056, Warner Instruments, Hamden, CT) to allow fine adjustment during the axial sciatic stretch. As described previously, the stretch steps consist of 5 s long ramped rising and returning phases to allow fine adjustment of the electrodes.

Pharmacological Targeting of K2P Channels. The effect of K2P channels on AP transmission is also assessed by local application of K2P agonist and antagonist to the sciatic nerve trunk during *in vitro* single-fiber recordings. The K2P agonist arachidonic acid (AA) was prepared by diluting the original liquid (ICN19462580, Fisher Scientific, East Greenwich, RI) in Krebs solution to 0.5 mM and 5 mM. The K2P antagonist ruthenium red (R2751-1G, Sigma Aldrich, Allentown, PA) was first dissolved to 10 mM stock in phosphate buffered saline and then diluted to 0.5 mM in Krebs solution. Both reagents were delivered to the sciatic nerve through a computer-controlled perfusion system (VCS-77, Warner Instruments, Hamden, CT) with a custom-pulled plastic barrel (PE-50, Warner Instruments, Hamden, CT) positioned ∼0.1 mm to the nerve trunk in the Krebs chamber. The flow of reagents was driven by gravity with an approximate flow rate of 100 μL/min. The complete process of each pharmacology test consists of 5 min baseline single-fiber recording, 15 min reagent application with concurrent single-fiber recording, and 25 min washout with Krebs solution. In the pharmacology-stretch experiments, the sciatic nerve underwent ascending steps of axial stretch (60 s step with 5 s ramped rising and returning phases, three steps of 1 mm, 2 mm, and 3 mm). The stepped stretch protocol was tested before, immediately after, and 25 min after (washout) the 15 min application of agonist AA or antagonist RR. The perfusion system uses multichannel valves to switch between the reagents and Krebs solution. This local reagent perfusion approach was validated by delivering 2% lidocaine, which reversibly blocks AP transmission in sciatic nerve axons.

Data Processing. APs were recorded extracellularly using a low-noise AC differential amplifier (DAM 80, World Precision Instruments, Sarasota, FL). The activity was monitored online, filtered (0.3−10 kHz), amplified (×10 000), digitized at 20 kHz using a 1401 interface (CED, Cambridge, U.K.), and stored on a PC. APs were discriminated off-line using Spike 2 software (CED). The root-mean-square (RMS) value of prestimulus noise was calculated, and 5 times that value was set as the detection threshold for AP spikes. The time at which the stimulus first exceeded the threshold was deemed as the onset of the AP. To avoid erroneous discrimination, we only studied single-unit APs temporarily separated from other neural activities by at least 3 ms in any record. CDs were measured as the time between the onset of stimulus artifact and the onset of recorded APs. CV was computed from the CD and the distance between stimulating and recording electrodes. Axial stretch was quantified by stretch ratio λ (i.e., the deformed nerve length divided by the *in vitro* nerve length at the zero-stretch state). The zero-stretch nerve length was measured as the distance between the proximal and distal ligatures (Figure 7A). Data were presented as the mean ± standard error (SE). Statistical analysis was performed using SigmaStat v4.0 (Systat Software, San Jose, CA). Differences were considered significant when $p < 0.05$.

AUTHOR INFORMATION

Corresponding Author

Bin Feng − *Department of Biomedical Engineering, University of Connecticut, Storrs, Connecticut 06269, United States;* orcid.org/0000-0001-9277-211X; Phone: 860-486-6435; Email: fengb@uconn.edu; Fax: 860-486-2500; https://npr.bme.uconn.edu

Authors

Jia Liu − *Department of Biomedical Engineering, University of Connecticut, Storrs, Connecticut 06269, United States*

Nishanth Ganeshbabu − *Department of Physiology and Neurobiology, University of Connecticut, Storrs, Connecticut 06269, United States*

Noha Shalaby − *Department of Biomedical Engineering, University of Connecticut, Storrs, Connecticut 06269, United States*

Longtu Chen − *Department of Biomedical Engineering, University of Connecticut, Storrs, Connecticut 06269, United States*

Tiantian Guo − *Department of Biomedical Engineering, University of Connecticut, Storrs, Connecticut 06269, United States*

Complete contact information is available at: https://pubs.acs.org/10.1021/acschemneuro.1c00052

Author Contributions

J.L., N.G., and B.F. conducted experiments. N.S., L.C., and T.G. critically reviewed and processed the experimental data. J.L., L.C., and B.F. prepared the display items. B.F. prepared the initial draft of the manuscript. All authors contributed to all aspects of manuscript preparation, revision, and editing. B.F. supervised the project.

Notes

The authors declare no competing financial interest.

ACKNOWLEDGMENTS

We sincerely thank Dr. G. F. Gebhart for editing the manuscript and providing constructive feedbacks. This work was supported by Grants NSF CAREER 1844762 and NIDDK R01 DK120824 awarded to B.F.

ABBREVIATIONS

AP, action potential; NRs, nodes of Ranvier; K2P, two-pore-domain potassium channel; CAP, compound action potential; CV, conduction velocity; CD, conduction delay; AA, arachidonic acid; RR, ruthenium red

REFERENCES

(1) Cuellar, J. M.; Alataris, K.; Walker, A.; Yeomans, D. C.; Antognini, J. F. Effect of high-frequency alternating current on spinal afferent nociceptive transmission. *Neuromodulation* **2013**, *16* (4), 318−27 (discussion 327).

(2) Masters, D. B.; Berde, C. B.; Dutta, S. K.; Griggs, C. T.; Hu, D.; Kupsky, W.; Langer, R. Prolonged regional nerve blockade by

controlled release of local anesthetic from a biodegradable polymer matrix. *Anesthesiology* **1993**, *79* (2), 340−6.
(3) Sarr, M. G.; Billington, C. J.; Brancatisano, R.; Brancatisano, A.; Toouli, J.; Kow, L.; Nguyen, N. T.; Blackstone, R.; Maher, J. W.; Shikora, S.; Reeds, D. N.; Eagon, J. C.; Wolfe, B. M.; O'Rourke, R. W.; Fujioka, K.; Takata, M.; Swain, J. M.; Morton, J. M.; Ikramuddin, S.; Schweitzer, M.; Chand, B.; Rosenthal, R.; The EMPOWER Study Group.. The EMPOWER Study: Randomized, Prospective, Double-Blind, Multicenter Trial of Vagal Blockade to Induce Weight Loss in Morbid Obesity. *Obes. Surg.* **2012**, *22* (11), 1771−1782.
(4) Waataja, J. J.; Tweden, K. S.; Honda, C. N. Effects of high-frequency alternating current on axonal conduction through the vagus nerve. *J. Neural Eng.* **2011**, *8* (5), 056013.
(5) Floras, J. S. Sympathetic nervous system activation in human heart failure: clinical implications of an updated model. *J. Am. Coll. Cardiol.* **2009**, *54* (5), 375−385.
(6) Gaunt, R. A.; Prochazka, A. Transcutaneously Coupled, High-Frequency Electrical Stimulation of the Pudendal Nerve Blocks External Urethral Sphincter Contractions. *Neurorehabilitation Neural Repair* **2009**, *23* (6), 615−626.
(7) Kanda, H.; Ling, J.; Tonomura, S.; Noguchi, K.; Matalon, S.; Gu, J. G. TREK-1 and TRAAK Are Principal K+ Channels at the Nodes of Ranvier for Rapid Action Potential Conduction on Mammalian Myelinated Afferent Nerves. *Neuron* **2019**, *104* (5), 960−971.
(8) Brohawn, S. G.; Wang, W.; Handler, A.; Campbell, E. B.; Schwarz, J. R.; MacKinnon, R. The mechanosensitive ion channel TRAAK is localized to the mammalian node of Ranvier. *eLife* **2019**, *8*, No. e50403.
(9) Enyedi, P.; Czirják, G. Molecular background of leak K+ currents: two-pore domain potassium channels. *Physiol. Rev.* **2010**, *90* (2), 559−605.
(10) La, J. H.; Gebhart, G. F. Colitis decreases mechanosensitive K2P channel expression and function in mouse colon sensory neurons. *Am. J. Physiol Gastrointest. Liver Physiol* **2011**, *301* (1), G165−G174.
(11) Feng, B.; Gebhart, G. F. Characterization of silent afferents in the pelvic and splanchnic innervations of the mouse colorectum. *Am. J. Physiol.: Gastrointest. Liver Physiol.* **2011**, *300* (1), G170−80.
(12) Chemin, J.; Patel, A. J.; Duprat, F.; Lauritzen, I.; Lazdunski, M.; Honore, E. A phospholipid sensor controls mechanogating of the K+ channel TREK-1. *EMBO J.* **2005**, *24* (1), 44−53.
(13) Maingret, F.; Lauritzen, I.; Patel, A. J.; Heurteaux, C.; Reyes, R.; Lesage, F.; Lazdunski, M.; Honore, E. TREK-1 is a heat-activated background K(+) channel. *EMBO J.* **2000**, *19* (11), 2483−91.
(14) Maingret, F.; Patel, A. J.; Lesage, F.; Lazdunski, M.; Honore, E. Mechano- or acid stimulation, two interactive modes of activation of the TREK-1 potassium channel. *J. Biol. Chem.* **1999**, *274* (38), 26691−6.
(15) Maingret, F.; Fosset, M.; Lesage, F.; Lazdunski, M.; Honore, E. TRAAK is a mammalian neuronal mechano-gated K+ channel. *J. Biol. Chem.* **1999**, *274* (3), 1381−7.
(16) Kang, D.; Choe, C.; Kim, D. Thermosensitivity of the two-pore domain K^+ channels TREK-2 and TRAAK. *J. Physiol.* **2005**, *564* (Part1), 103−116.
(17) Noël, J.; Zimmermann, K.; Busserolles, J.; Deval, E.; Alloui, A.; Diochot, S.; Guy, N.; Borsotto, M.; Reeh, P.; Eschalier, A.; Lazdunski, M. The mechano-activated K+ channels TRAAK and TREK-1 control both warm and cold perception. *EMBO J.* **2009**, *28* (9), 1308−1318.
(18) Stecker, M. M.; Baylor, K. Peripheral nerve at extreme low temperatures 1: effects of temperature on the action potential. *Cryobiology* **2009**, *59* (1), 1−11.
(19) Paintal, A. S. Block of conduction in mammalian myelinated nerve fibres by low temperatures. *J. Physiol.* **1965**, *180* (1), 1−19.
(20) Klumpp, D.; Zimmermann, M. Irreverisble differential block of A- and C-fibres following local nerve heating in the cat. *J. Physiol.* **1980**, *298* (1), 471−482.
(21) Hoogeveen, J. F.; Troost, D.; Van Der Kracht, A. H. W.; Wondergem, J.; Haveman, J.; Gonzalez, D. G. Ultrastructural changes in the rat sciatic nerve after local hyperthermia. *Int. J. Hyperthermia* **1993**, *9* (5), 723−730.
(22) Zhang, Z.; Lyon, T. D.; Kadow, B. T.; Shen, B.; Wang, J.; Lee, A.; Kang, A.; Roppolo, J. R.; de Groat, W. C.; Tai, C. Conduction block of mammalian myelinated nerve by local cooling to 15−30°C after a brief heating. *J. Neurophysiol.* **2016**, *115* (3), 1436−1445.
(23) Kwan, M. K.; Wall, E. J.; Massie, J.; Garfin, S. R. Strain, stress and stretch of peripheral nerve. Rabbit experiments in vitro and in vivo. *Acta Orthop. Scand.* **1992**, *63* (3), 267−72.
(24) Li, J.; Shi, R. A device for the electrophysiological recording of peripheral nerves in response to stretch. *J. Neurosci. Methods* **2006**, *154* (1), 102−108.
(25) Li, J.; Shi, R. Stretch-induced nerve conduction deficits in guinea pig ex vivo nerve. *J. Biomech.* **2007**, *40* (3), 569−578.
(26) Rickett, T.; Connell, S.; Bastijanic, J.; Hegde, S.; Shi, R. Functional and Mechanical Evaluation of Nerve Stretch Injury. *J. Med. Syst.* **2011**, *35* (5), 787−793.
(27) Wall, E. J.; Massie, J. B.; Kwan, M. K.; Rydevik, B. L.; Myers, R. R.; Garfin, S. R. Experimental stretch neuropathy. Changes in nerve conduction under tension. *J. Bone Jt. Surg., Br. Vol.* **1992**, *74-B* (1), 126−129.
(28) Ruscheweyh, R.; Forsthuber, L.; Schoffnegger, D.; Sandkühler, J. J. J. o. C. N. Modification of classical neurochemical markers in identified primary afferent neurons with Aβ-, Aδ-, and C-fibers after chronic constriction injury in mice. *J. Comp. Neurol.* **2007**, *502* (2), 325−336.
(29) Li, C.; Bak, A. J. E. n. Excitability characteristics of the A-and C-fibers in a peripheral nerve. *Exp. Neurol.* **1976**, *50* (1), 67−79.
(30) Chen, L.; Ilham, S. J.; Guo, T.; Emadi, S.; Feng, B. In vitro multichannel single-unit recordings of action potentials from mouse sciatic nerve. *Biomed. Phys. Eng. Express* **2017**, *3* (4), 045020.
(31) Ilham, S. J.; Chen, L.; Guo, T.; Emadi, S.; Hoshino, K.; Feng, B. In vitro single-unit recordings reveal increased peripheral nerve conduction velocity by focused pulsed ultrasound. *Biomed. Phys. Eng. Express* **2018**, *4* (4), 045004.
(32) Lundborg, G.; Rydevik, B. Effects of stretching the tibial nerve of the rabbit. A preliminary study of the intraneural circulation and the barrier function of the perineurium. *J. Bone Jt. Surg., Br. Vol.* **1973**, *55-B* (2), 390−401.
(33) Jou, I.-M.; Lai, K.-A.; Shen, C.-L.; Yamano, Y. Changes in conduction, blood flow, histology, and neurological status following acute nerve-stretch injury induced by femoral lengthening. *J. Orthop. Res.* **2000**, *18* (1), 149−155.
(34) Patel, A. J.; Honoré, E.; Maingret, F.; Lesage, F.; Fink, M.; Duprat, F.; Lazdunski, M. A mammalian two pore domain mechano-gated S-like K+ channel. *EMBO J.* **1998**, *17* (15), 4283−4290.
(35) Taha, A. M.; Abd-Elmaksoud, A. M. Lidocaine use in ultrasound-guided femoral nerve block: what is the minimum effective anaesthetic concentration (MEAC90)? *Br. J. Anaesth.* **2013**, *110* (6), 1040−1044.
(36) Gerhart, D. Z.; Drewes, L. R. Glucose transporters at the blood-nerve barrier are associated with perineurial cells and endoneurial microvessels. *Brain Res.* **1990**, *508* (1), 46−50.
(37) Feng, B.; Kiyatkin, M. E.; La, J.-H.; Ge, P.; Solinga, R.; Silos-Santiago, I.; Gebhart, G. F. Activation of Guanylate Cyclase-C Attenuates Stretch Responses and Sensitization of Mouse Colorectal Afferents. *J. Neurosci.* **2013**, *33* (23), 9831−9839.
(38) Feng, B.; Zhu, Y.; La, J. H.; Wills, Z. P.; Gebhart, G. F. Experimental and computational evidence for an essential role of NaV1.6 in spike initiation at stretch-sensitive colorectal afferent endings. *J. Neurophysiol.* **2015**, *113* (7), 2618−34.
(39) Plonsey, R.; Barr, R. C. *Bioelectricity: A Quantitative Approach*; Springer Science & Business Media, 2007; pp 155−186.
(40) Tavee, J.; Zhou, L. Small fiber neuropathy: a burning problem. *Cleveland Clin. J. Med.* **2009**, *76* (5), 297−305.
(41) Feng, B.; La, J. H.; Schwartz, E. S.; Gebhart, G. F. Irritable bowel syndrome: methods, mechanisms, and pathophysiology. Neural and neuro-immune mechanisms of visceral hypersensitivity in irritable

https://doi.org/10.1021/acschemneuro.1c00052
ACS Chem. Neurosci. 2021, 12, 3558−3566

bowel syndrome. *Am. J. Physiol.: Gastrointest. Liver Physiol.* **2012**, *302* (10), G1085−98.
(42) Schaible, H. G.; Ebersberger, A.; Von Banchet, G. S. Mechanisms of pain in arthritis. *Ann. N. Y. Acad. Sci.* **2002**, *966* (1), 343−354.
(43) Yoshimura, N.; Oguchi, T.; Yokoyama, H.; Funahashi, Y.; Yoshikawa, S.; Sugino, Y.; Kawamorita, N.; Kashyap, M. P.; Chancellor, M. B.; Tyagi, P.; Ogawa, T. Bladder afferent hyperexcitability in bladder pain syndrome/interstitial cystitis. *Int. J. Urol.* **2014**, *21*, 18−25.
(44) Brumovsky, P. R.; Feng, B.; Xu, L.; McCarthy, C. J.; Gebhart, G. F. Cystitis increases colorectal afferent sensitivity in the mouse. *Am. J. Physiol.: Gastrointest. Liver Physiol.* **2009**, *297* (6), G1250−8.
(45) Feng, B.; Gebhart, G. F. In vitro functional characterization of mouse colorectal afferent endings. *J. Visualized Exp.* **2015**, *95*, 52310.
(46) Feng, B.; Joyce, S. C.; Gebhart, G. F. Optogenetic activation of mechanically insensitive afferents in mouse colorectum reveals chemosensitivity. *Am. J. Physiol.: Gastrointest. Liver Physiol.* **2016**, *310* (10), G790−8.

https://doi.org/10.1021/acschemneuro.1c00052
ACS Chem. Neurosci. 2021, 12, 3558−3566